Indications of phase separation in polycrystalline $La_{1-x}Sr_xMnO_3$ for $x \approx 0.5$

S. I. Patil,* S. M. Bhagat, Q. Q. Shu,† S. E. Lofland,‡ S. B. Ogale, V. N. Smolyaninova, X. Zhang, B. S. Palmer, R. S. Decca, F. A. Brown,§ H. D. Drew, and R. L. Greene
Department of Physics, University of Maryland, College Park, Maryland 20742-4111

I. O. Troyanchuk
National Academy of Science of Belarus, Institute of Solid State Physics, P. Brovki 17, Minsk 220072, Belarus

W. H. McCarroll
Department of Chemistry and Biochemistry, Rider University, Lawrenceville, New Jersey 08648-3099
(Received 20 August 1999; revised manuscript received 20 April 2000)

We present systematic studies of polycrystalline $La_{1-x}Sr_xMnO_3$ where x is varied from 0.46 to 0.53 at 0.01 intervals. We have measured the magnetic resonance, ac susceptibility, dc magnetization, x-ray diffraction, four-probe resistivity, and optical reflectivity. The data seem to indicate that, at low T, the materials are intimate mixtures of ferromagnetic and antiferromagnetic microregions. For $x > 0.48$ we observe anomalies pointing toward charge ordering on lowering T. An effective-medium theory is presented, and an appropriate phase diagram is proposed.

I. INTRODUCTION

It is generally recognized that the manganites $R_{1-x}A_xMnO_3$, where R is a rare earth such as La, Nd, etc., and A an alkaline earth like Sr, Ba, or Ca, exhibit a very rich phase diagram because of subtle competition among interactions involving spin, lattice, and charge degrees of freedom. All the energy scales appear to be comparable so that modest variations in the dopant concentration, preparation method, local chemistry, cation deficiency, etc., can cause profound changes in (i) the magnetic state—ferromagnetic (FM), antiferromagnetic (AFM), canted FM, canted AFM; (ii) the transport properties: dirty metal, insulator, semiconductor, polaron hopping; and (iii) the structural characteristics: Jahn-Teller-induced strains, orthorhombic to rhombohedral transformations. They also exhibit a remarkable sensitivity to magnetic fields—colossal magnetoresistance, field-dependent structural phase transitions, and the like. No brief summary can provide an accurate description of all the observations. A recent review is due to Coey *et al.*[1]

In some sense, the $La_{1-x}Sr_xMnO_3$ $(0.3 < x < 0.5)$ system is among the simplest. The resistivity ρ is metal-like, $(d\rho/dT) > 0$ and $\rho < 1$ mΩ cm, over wide ranges of temperature T and exhibits a modest drop when T is lowered through the ordering temperature T_C.[2] Although the theories are not completely satisfactory, the conventional wisdom is that the e_g bandwidth is quite large so that the kinetic energy or equivalently double exchange wins out. The phase diagram, using single-crystal samples, has been established for some time.

However, it must be noted ferromagnetic resonance (FMR) studies[3,4] indicate that most samples (including single crystals) are *magnetically inhomogeneous*. Also, optical measurements[5] show unexpected sensitivity to surface preparation for presumably the same material. Further systematic studies are needed.

To be precise, materials with x close to 0.5, which are the focus of the present study, have been found to show marked differences depending on the crystalline state. Using single crystals, Moritomo *et al.*[6] found that for $x \approx 0.5$, the high-temperature paramagnetic (PM) metal becomes a FM metal but with a somewhat suppressed magnetic moment (see below). Furthermore, AFM behavior appeared only when $x \geqslant 0.54$. However, Fujishiro *et al.*,[7] using polycrystalline samples, reported that $La_{1-x}Sr_xMnO_3$ with $x = 0.48$, 0.50, and 0.52, exhibit resistivity and acoustic anomalies usually attributed to onset of charge ordering (CO). In the present work, it was decided to make a thorough study of polycrystalline $La_{1-x}Sr_xMnO_3$, near $x = 0.5$, by varying the Sr content from 0.46 to 0.53 at 0.01 intervals. Accordingly, we have measured the ferromagnetic resonance (FMR), ac susceptibility, dc magnetization, electrical resistance in zero field and with an applied field of 85 kOe, x-ray diffraction, inductively coupled plasma analysis, and circularly polarized light reflectivity.

It turns out that the observed properties are remarkably sensitive to x. For instance, whereas $x = 0.46$ and 0.47 are FM down to the lowest T, 0.48 exhibits a Néel temperature T_N of ≈ 100 K. In addition, we report several interesting findings: (i) as in Ref. 6 the FM-state magnetization is well below that corresponding to full alignment of the spins and drops rapidly with increasing x; (ii) a proper understanding of the field for FMR requires spin-wave-like contributions pointing to the existence of FM clusters in an AFM background;[8] (iii) although there is no activated regime, the resistivity ρ shows a CO-like step, which is sensitive to applied magnetic fields; (iv) over wide ranges of temperature, ρ varies linearly with T. It seems reasonable to propose that this be understood in terms of an effective medium theory in which, on lowering T, an increasing fraction of the sample goes into an insulating (presumably CO) phase; (v) for $x > 0.48$, the optical conductivity becomes anisotropic as T is lowered through the regime where R shows a step, a possible indicator of onset of CO in some grains. Although many

details can only be settled after considerable further study, it is important to note that these observations already provide ample evidence that in the neighborhood of $x \approx 0.5$, not only other manganites but also polycrystalline $La_{1-x}Sr_xMnO_3$ is unstable against fluctuations so that instead of having a uniform and homogeneous magnetic ground state, the low-T phase is an intimate mixture of FM, AFM, and perhaps CO regions in the grains of the ceramic sample. Preliminary FMR measurements on a single crystal of $La_{0.5}Sr_{0.5}MnO_3$ show indications of magnetic fractionation [as in (ii) above]. Full details will be reported elsewhere. A possible explanation for the differences between single crystals and ceramics is the presence of large strains in the lattice of the micron-size grains.

II. METHODS

Polycrystalline samples of $La_{1-x}Sr_xMnO_3$ were prepared via the standard solid-state reaction route starting from high-purity ($>99.99\%$) La_2O_3, $SrCO_3$, and Mn_3O_4. The powders were mixed, finely ground, and sintered at 900 °C for 20 h. The grinding and sintering steps were repeated at 1000 °C for 20 h, 1100 °C for 20 h, and 1160 °C for 40 h. After pelletization, the final sintering was carried out at 1400 °C for 40 h, respectively. Increasing this time to 120 h enhanced the sample density for Sr0.51 by $\approx 10\%$ but did not affect the transition temperatures discussed below. Typical grain size is $3-5$ μm.

Immediately after the sample was prepared, x-ray diffractometry was done to establish that it was single phase, at the 5% level. The following properties have been measured over wide temperature intervals: (a) low-field (≈ 8 Oe) ac susceptibility χ_{ac}; (b) ferromagnetic resonance; (c) self-field (demagnetizing field) at the sample surface using an electron paramagnetic resonance probe; (d) dc magnetization using superconducting quantum interference device magnetometry at fields up to 50 kOe; and (e) four-probe electrical resistance in zero field and an applied field of 85 kOe, parallel to the current direction. Further, using a narrowly focused ($\approx$ few μm^2) beam, the reflection of circularly polarized light, from a single grains of the ceramic sample, was measured from room temperature down to 77 K. The degree of ellipticity in the reflected light provides a straightforward measure of any anisotropy in the optical conductivity. Such measurements have been used previously to mark the onset of CO in manganite samples.[9–12]

Inductively coupled plasma analysis, titration, and more detailed x-ray studies of some of the samples, reveal La deficiencies of a few percent and unreacted material at $\leqslant 1\%$ level. However, the relative Sr concentrations are quite reliable. Thus, for the present discussion, we choose to label the samples by their nominal Sr content; i.e., $La_{1-x}Sr_xMnO_3$ is designated as Srx.

III. RESULTS AND DISCUSSION

We begin by cataloging all the experimental findings and at the end propose a phase diagram and a qualitative picture to account for the variety of behaviors consequent on variation of x, applied field, and temperature.

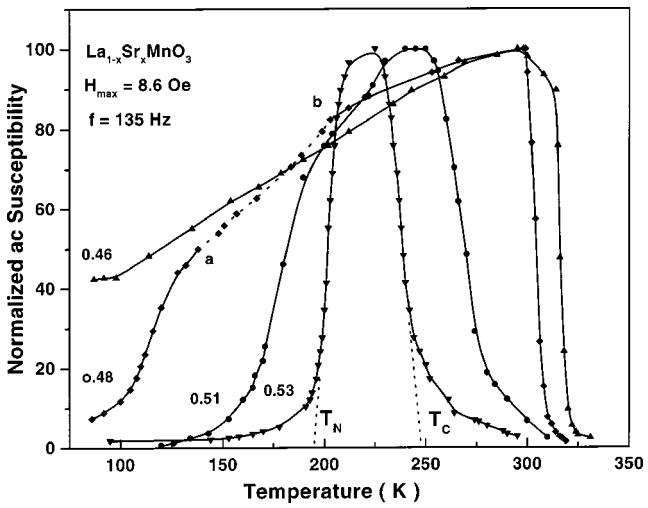

FIG. 1. Low-field normalized ac susceptibility vs temperature. With increasing x, T_C drops and T_N increases. The ab region (dotted) delineates the temperature interval of the resistive anomaly due to CO.

A. ac susceptibility

Since the output of the locally built susceptometer depends on sample size and shape, we have normalized the data to the maximal value in each case and displayed the temperature dependence in Fig. 1. The PM-FM transition is marked by a sharp increase in χ_{ac} as T is lowered. The transitions are not particularly sharp and get less so with increasing x. As shown, T_C is obtained by extrapolating the region of sharp rise of χ_{ac}. In the Sr0.46 and Sr0.47 samples χ_{ac} reduces somewhat as T is lowered. This is as expected for a FM because the increasing magnetization forces the sample to adopt a domain structure with ever smaller domain sizes. However, for $x \geqslant 0.48$, χ_{ac} shows a sharp drop at low T, and this is interpreted as delineating the onset of antiferromagnetism. Again, T_N is located by extrapolating the χ_{ac} vs. T curve. In addition, it is notable that χ_{ac} exhibits a broad dip (see region ab for the Sr0.48 curve) in the same T interval where the resistivity has a step and the optical conductivity becomes anisotropic.

B. Electron-spin resonance

The electron-spin resonance was studied at both $T > T_C$ (electron paramagnetic resonance, EPR) and $T < T_C$ (ferromagnetic resonance, FMR) at several frequencies between 8 and 34 GHz. Apart from noting that the EPR gives $g \approx 2$ in every case, here we will discuss only the FMR data. (i) The FMR lines are quite wide, and in some cases there are several lines present. Even in Sr0.46 and Sr0.47 one cannot follow the signal at temperatures below about $T_C - 100$ K as the linewidth becomes several kOe. As before,[3,4] this is a clear indication of the magnetic inhomogeneity which attends nearly all manganite samples. (ii) The room-temperature 10.45 GHz spectrum observed in a parallelepiped ($2 \times 3 \times 9$ mm with H parallel to the long axis) of Sr0.46 is shown in Fig. 2. The data were taken using an FMR microscope[13] so that only ≈ 1 mm^2 of one broad face was exposed to microwaves. As expected for a thick conductor, one observes a ferromagnetic antiresonance (FMAR, where

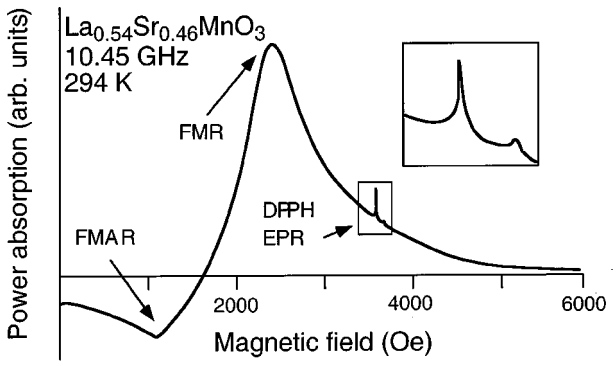

FIG. 2. Spin-resonance spectrum indicating FMAR and FMR. The sharp lines (see inset) near $g=2$ represent PM markers used to measure the local field (see text, Fig. 6).

the dynamic permeability vanishes) at about 1.1 kOe and an FMR at about 2.4 kOe. The half width is ≈ 1 kOe. The two sharp lines near $g \approx 2$ come from PM markers (2,2-Diphenyl-1-Picrylhydrazyl, DPPH), one of which is located on the sample surface and the other about 2 cm away. Their field separation is a direct measure of the demagnetizing field H_d (≈ 100 Oe in Fig. 2). For a disk-shaped sample the FMAR field is given by $H_{\mathrm{FMAR}}=(\omega/\gamma-4\pi M)$ where M is the magnetization. Taking $g=2$ and H_d into account one gets $4\pi M=2.7$ kOe, well in accord with the dc data at a comparable applied field. These values, however, will not account for the observed FMR field H_{FMR}. The shortfall of ≈ 250 Oe may be explained if the FMR equation has a spin wave contribution; i.e., there is an exchange field $(Dq^2/\gamma\hbar)$ where D is the spin-wave stiffness and γ the gyromagnetic ratio, augmenting the applied field, yielding

$$\left(\frac{\omega}{\gamma}\right)^2=\left(H_{\mathrm{FMR}}+\frac{Dq^2}{\gamma\hbar}\right)\left(H_{\mathrm{FMR}}+\frac{Dq^2}{\gamma h}+4\pi M\right). \quad (1)$$

Using $D=100$ meV Å^2, which is typical for a manganite, one would conclude that the effective wavelengths are about 1200 Å. If so, the 10-GHz FMR data help to define a different length in these compounds; i.e., the FM regions are about 600 Å in extent. At 294 K, the effective exchange field reduces rapidly as one goes from Sr0.46 to Sr0.48. This is as expected because D should reduce as one gets close to T_C. In any case, the 10-GHz FMR measurements seem to be revealing the length scale of the magnetic inhomogeneity to be a few hundred Å, much smaller than the typical grain size of ≈ 3–5 microns. It is instructive to mention that at 34 GHz there is a smaller discrepancy if the parameters derived from H_{FMAR} are used to calculate H_{FMR}. Presumably, the large applied dc fields (≈ 10 kOe) needed for resonance at 34 GHz are helping to enhance the size of the FM regions thereby suppressing the exchange contributions.

As noted above, by measuring the field separation between two EPR lines from the DPPH markers (inset, Fig. 2), one can access the effective demagnetizing field and compare it with that expected from a uniformly magnetized FM parallelepiped. In the FM region the observed and calculated H_d values are in very good agreement. The surprise is that even at low T, when one is well inside the AFM region, H_d appears to be due to a uniformly magnetized FM sample

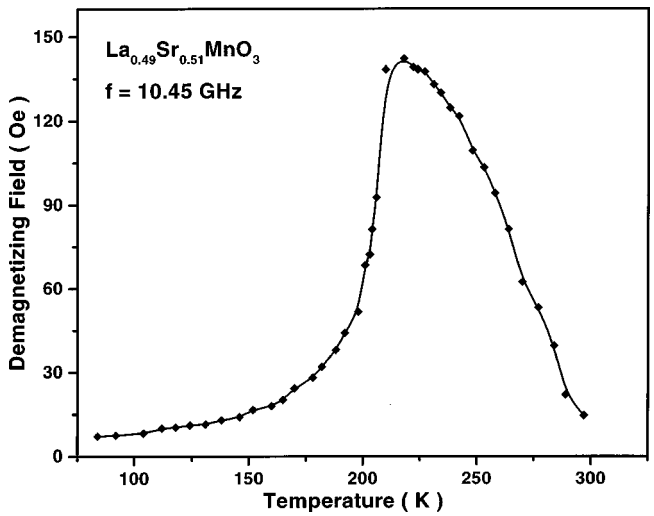

FIG. 3. Demagnetizing field at sample surface. The low-temperature behavior shows that the FM moment is spread uniformly throughout the sample.

(Fig. 3). That is, the FM component appears to pervade the entire volume of the sample. Admittedly, dipole fields are long range, but if the sample were divided into well separated FM and AFM regions, H_d would no longer be given by the simple parallelepiped formula. The material is indeed an intimate mixture of FM and AFM microdomains. The FMR data thus suggest that polycrystalline $La_{1-x}Sr_xMnO_3$ with $x \approx 0.5$ is rather similar to $La_{0.5}Ca_{0.5}MnO_3$ where high-resolution lattice images by Mori *et al.*[14] and nuclear magnetic resonance studies by Allodi *et al.*[15] have been used to reveal such coexisting magnetic phases at low T.

The results are similar to what others have found in the La-Ca (Refs. 16 and 17) and Nd-Sr (Ref. 18) systems and could be used to support the phase-separation scenarios of Moreo *et al.*[19] They also lend credence to the mixed FM-AFM models proposed by Nagaev.[20]

C. dc magnetization

Figure 4 shows the temperature dependence of the dc magnetization M in a field of 10 kOe for a few representative cases. It is notable that (i) Sr0.46 and Sr0.47 (not shown) remain FM down to the lowest T; (ii) Sr0.46 has the highest zero-Kelvin magnetization, which corresponds to $2.5\mu_B$ per Mn ion, which is much smaller than the $3.5\mu_B$ expected from complete alignment. As noted above, single-crystal specimens show a similar deficiency.[6] There are two possibilities for this short fall—all the Mn ions do not participate in the ferromagnetism, rather some of them have antiferromagnetic (AFM) coupling, or there is spin canting. It is felt that the former is the more likely scenario, because (iii) the magnetizations of Sr0.48–Sr0.53 all show a sharp decline at low T, symptomatic of the onset of predominantly AFM alignment. (iv) At low T, however, there is still a sizable nonzero magnetization indicating that well below T_N, there is a considerable FM component in the material. (v) At ≈ 50 K, there is a small jog in the M vs T curve. This is the same temperature at which the T dependence of ρ changes slope (cf. Fig. 5). The magnetization data again support the mixed FM-AFM phase picture implied by the resonance measurements.

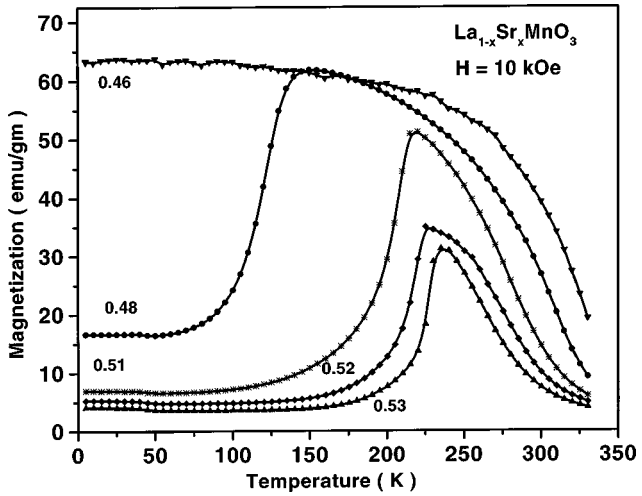

FIG. 4. dc magnetization in 10-kOe field. In the FM region, the maximal moment is $2.3\mu_B$ compared to $3.5\mu_B$ expected for full alignment. Note that the magnetization is nonzero even for T well below T_N.

D. Electrical transport

The operational magnitude of the electrical resistivity was obtained from the measured resistance by assuming that the current distribution is uniform. The results are shown in Fig. 5 and are best summarized as follows: (i) for Sr0.46–0.50, $\Delta\rho/\Delta T$ is positive in the PM region, the resistivity is metallic; (ii) at higher x, $\Delta\rho/\Delta T$ is negative at high T as well; (iii) for Sr0.46–0.50, ρ exhibits the expected drop accompanying the onset of ferromagnetism in the manganites (see inset in Fig. 5 for Sr0.50); (iv) for Sr0.48–Sr0.53, ρ shows a step on reducing T. The sharpness of the step is well delineated by the derivative curve in the inset of Fig. 5. This transition region is nearly 40 K wide in Sr0.48 but becomes considerably narrower (≈ 10 K) in Sr0.53. It coincides roughly with the region of the $\chi_{\rm ac}$ anomaly (ab) in Fig. 1. As we shall see, the optical reflectivity measurements indicate the onset of an anisotropy in the conductivity at a comparable temperature. This leads us to propose that the step is related to the appearance of CO in some grains of the sample. Hence the label $T_{\rm CO}$ in the inset of Fig. 5. (v) However, at lower T, ρ fails to rise exponentially as would be expected if the CO state prevailed everywhere. Rather, ρ exhibits a linear rise with reducing T. In Sr0.46 and Sr0.47, ρ can be described by writing, roughly,

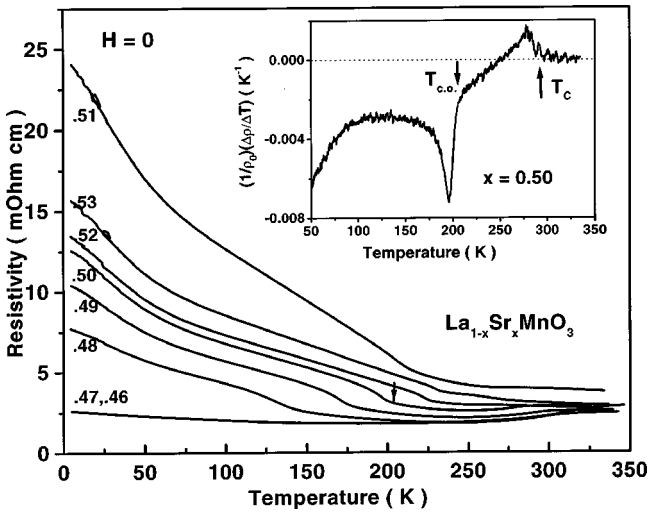

FIG. 5. Zero-field resistivity vs T. For $x \geqslant 0.48$, the step in ρ suggests the onset of CO, yet the low-T state is not truly insulating. The inset shows $\Delta\rho/\Delta T$ is constant [Eq. (2)] for $T < T_{\rm CO}$.

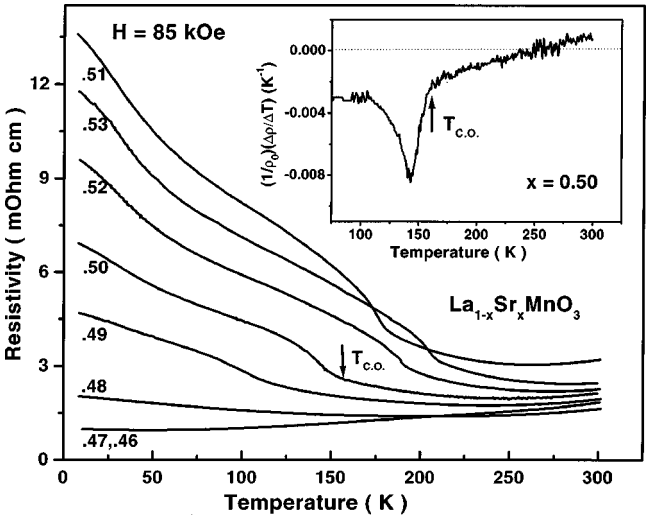

FIG. 6. Resistivity in 85 kOe. All the CO anomalies are shifted to lower temperature (cf. Fig. 5)

$$\rho = \rho_0\left[1 - \frac{T}{(320 \pm 50)\,\mathrm{K}}\right] \tag{2}$$

with $T < 70$ K and $\rho_0 \approx 2$–5 mΩ cm. The slight increase in ρ below 70 K is most likely caused by the magnetic fractionation, i.e., progressive breakdown of the homogeneous FM phase. On the other hand, for Sr0.48–Sr0.53 the low-T variation is more marked and follows

$$\rho = \rho_0\left[1 - \frac{T}{(290 \pm 40)\,\mathrm{K}}\right] \quad \text{for} \quad 50\ \mathrm{K} < T \leqslant T_{\rm CO} \tag{3a}$$

and

$$\rho = \rho_0'\left[1 - \frac{T}{(160 \pm 10)\,\mathrm{K}}\right] \quad \text{for} \quad T < 50\ \mathrm{K}. \tag{3b}$$

Below, an attempt will be made to account for Eqs. (3a) and (3b) in terms of an effective medium theory. (vi) The 4-K value of ρ is not monotonic in x. It has its largest value for Sr0.51. However, it reaches only 25 mΩ cm, which is orders of magnitude smaller than what would be obtained by charge ordering of all the (Mn^{3+}, Mn^{4+}) pairs.

Figure 6 shows the temperature dependence of the effective resistivity in the presence of a longitudinal field of 85 kOe. The data shown are for the field-cooled state. However, there is only a slight thermal hysteresis in the region of the resistive anomaly. We note that (i) the low T rise in ρ for Sr0.46 and Sr0.47 is largely suppressed, $\Delta\rho/\Delta T$ is weakly positive at all T; the field promotes FM alignment everywhere; (ii) the transport anomaly in Sr0.48 has been driven to $T < 4$ K; (iii) in every case the temperature of the onset of the anomaly shifts down with applied field, but the shift reduces from 150 K for Sr0.48 to ≈ 20 K for Sr0.53. (iv) For Sr0.49–Sr0.52 the slope of the low-T linear rise is rather

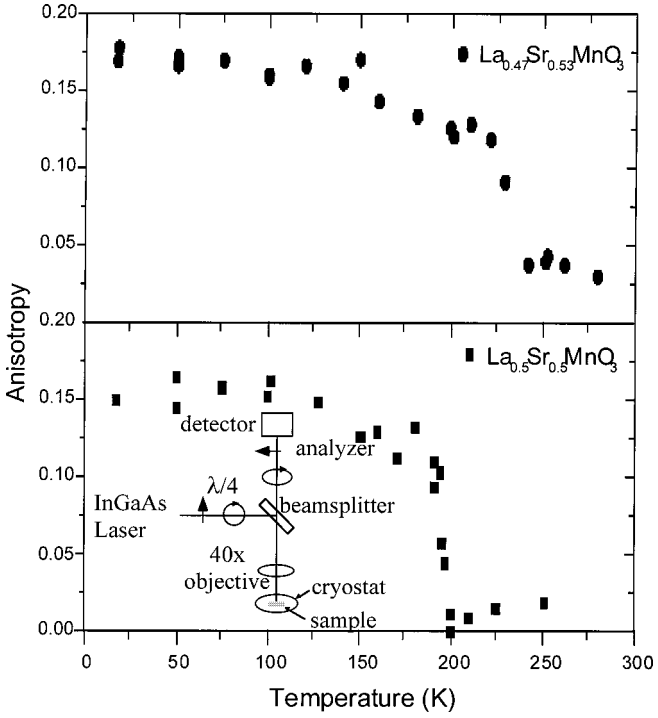

FIG. 7. Temperature dependence of the optical anisotropy for Sr0.53 and Sr0.50. Note the onset of the anisotropy coincides with the temperature for which the resistivity has an abrupt increase. The inset shows the experimental setup.

insensitive to H. (v) $\rho_0'(85\ \text{kOe})$ is highest for Sr0.51. (vi) The largest MR $\{=[\rho(85\ \text{kOe})-\rho(0)]/\rho(0)\}$ value is 70% at 25 K for Sr0.48.

E. Reflectivity

Further evidence for the existence of a ''charge ordered'' phase in the material is provided by optical measurements on facets of single grains of the sintered pellets. For two-dimensional charge ordering such as has been observed in other CMR alloys the optical conductivity becomes anisotropic.[9–12] Therefore the reflectance differs for light polarized parallel and perpendicular to the planes. To obtain information from an individual grain of the sintered sample, circularly polarized light ($\lambda=1.55\ \mu$m) from an InGaAs diode laser was focused onto the sample by means of a microscope objective (N.A. = 0.55) which gave a spot size of $\approx 1.2\ \mu$m. The 1.55-μm radiation was chosen because the optical anisotropy of $Pr_{1-x}Ca_xMnO_3$ ($x=0.4$) and $Bi_{1-x}Ca_xMnO_3$ ($x>0.5$) was reported to be larger in the infrared.[9–12] The reflected light was collected through the same microscope objective and passed through an analyzer to measure the ellipticity of the reflected light. In what follows, the anisotropy of the signal $A=(I_M-I_m)/(I_M+I_m)$ where I_M (I_m) is the maximum (minimum) intensity measured at the detector when rotating the analyzer. With this definition circular polarized light would have an anisotropy of zero and linear polarized light would have an anisotropy of one.

Figure 7 shows a typical data set for Sr0.53 and Sr0.5 where the anisotropy A is graphed as a function of temperature. At low temperatures the ellipticity of the reflected light

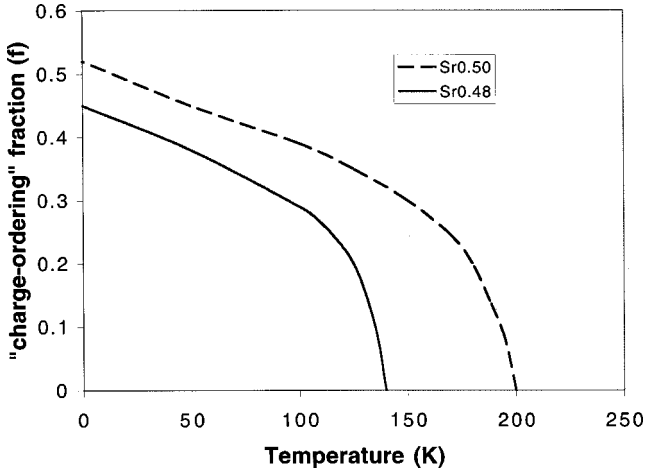

FIG. 8. Calculated ''charge ordering'' fraction as ascertained from Eq. (5).

from some of the facets has increased where the crossover temperature is the ''charge ordering temperature.'' The onset of anisotropy for the Sr0.53 sample occurs at 230 and 195 K for the Sr0.5 sample. These temperatures agree well with the ''charge ordering'' critical temperature measured by the jump in the resistivity. The Sr0.46 grains do not exhibit any measurable change in the optical anisotropy at any temperature between 20 and 280 K, consistent with the resistivity and magnetization data. That only some facets show the effect is consistent with charge ordering in a particular plane in which case only two-thirds of the facets should by optically anisotropic.

It was found that the optical anisotropy effect had more complex behavior for larger grains ($>30\ \mu$m). This observation is interpreted in terms of the presence of domains with different ''charge ordering planes'' in the larger crystallites.

F. Effective-medium picture

Both the optical and transport data yield results similar to those consequent on charge ordering. Indeed, charge ordered materials invariably display optical anistropy, whose onset, in the present samples coincides with the resistive anomaly. Further evidence comes from the shift in the step temperature on application of a field. Recall that similar shifts are observed in CO transitions in other manganites. However, as noted above, the present system is never truly an insulator. Thus one cannot call this a case of uniform charge ordering. In order to reconcile all the observations, it seems reasonable to propose that below T_{CO} the sample is an intimate mixture of CO (essentially insulating) and conducting regions with the fraction of the former increasing as T is reduced. Such models have been considered before by Kim *et al.*[21] and Chun *et al.*[22]

Let us consider a simple effective-medium approach. For a two-component system, one writes[23]

$$f\,\frac{\sigma_1-\sigma_{\text{eff}}}{\sigma_1+2\sigma_{\text{eff}}}+(1-f)\,\frac{\sigma_2-\sigma_{\text{eff}}}{\sigma_2+2\sigma_{\text{eff}}}=0, \tag{4}$$

where f is the volume fraction of component 1, σ_1 and σ_2 the conductivity of the first and second component, respec-

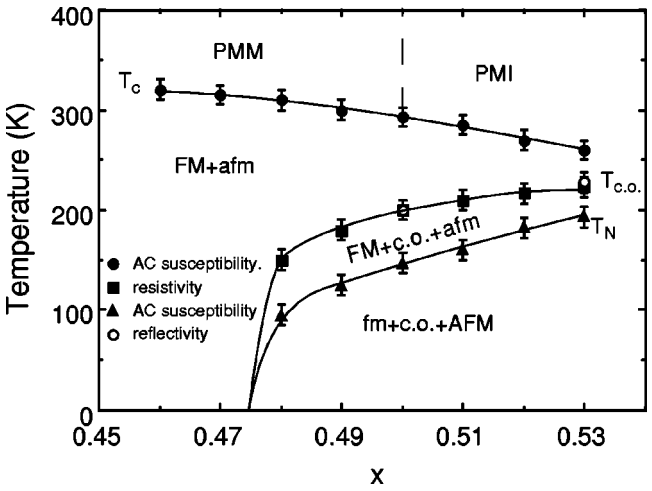

FIG. 9. Proposed phase diagram of $La_{1-x}Sr_xMnO_3$ showing coexistence of FM, AFM, and CO phases. I stands for insulator and M for metal. The capital letters indicate the predominant phase while the lowercase letters are for the minority phase.

tively, and σ_{eff} the effective conductivity of the mixture. For simplicity let us assume that the conducting regions have a temperature-independent resistivity ρ_0, as seems to be nearly the case for Sr0.46 and Sr0.47. Additionally, let us suppose that the charge carriers in the CO regions are completely localized; i.e., their conductivity is 0. For this particular two-component system, one finds that the fraction of CO is

$$f=\frac{\rho-\rho_0}{3\rho}. \tag{5}$$

This is shown in Fig. 8 for Sr0.48.

Thus the magnetic and transport data suggest that as x comes close to 0.5, first there is magnetic fragmentation (in 0.46–0.47) where a predominantly FM phase gives way to some AFM inclusions, next the AFM becomes more predominant, CO makes its appearance and causes a step in ρ and more marked rise in ρ at low T.

IV. PHASE DIAGRAM AND CONCLUSIONS

We propose for polycrystalline $La_{1-x}Sr_xMnO_3$ for $x \approx 0.5$ the phase diagram shown in Fig. 9. At T_C there is an onset of FM ordering, but the FM state does not encompass every spin. Rather, there is a significant fraction of antiferromagnetically coupled spins present. That is, for $T_C > T > T_{CO}$ the system is composed of FM and AFM regions. At T_{CO}, charge ordering occurs in some parts of the sample, the resistivity jumps, but once again, the CO does not involve all the (Mn^{3+},Mn^{4+}) pairs. For $T_{CO} > T > T_N$, FM, AFM, and CO all exist side by side. At T_N, antiferromagnetism begins to take over, but the FM fraction does not vanish even at 4 K. To summarize, below T_C we have FM and AFM correlations coexisting with the FM predominant; below T_{CO} the state is an intimate mixture of FM, AFM, and CO phases with predominant FM couplings; and finally below T_N, AFM, FM, and CO coexist but in a predominantly AFM material.

In attempting to reconcile the properties and phase diagram of $La_{1-x}Sr_xMnO_3$ for $x \approx 0.5$ for single crystals with those observed here, one should note the following. First, as far as the low-T magnetic state is concerned, it appears that there are quantitative rather than qualitative discrepancies. In both cases the FM magnetization is well below that expected of full alignment. As before FMR data continue to point to magnetic inhomogeneities. However, the present measurements demonstrate that one can get a handle on the state of inhomogeneity. Studies on other manganites are underway to check if similar estimates can be made. Second, when we come to the transport anomalies, it has to be noted that the grains in the sintered material are quite heavily strained. A cursory glance at the lines in the x-ray-diffraction pattern shows widths of greater than 0.5° rather than the 0.1° found for single crystals. This will almost certainly lower the symmetry and may promote a CO state in some of the worst affected grains.[24]

ACKNOWLEDGMENTS

We thank A. Chattopadhyay and J. Gopalakrishnan for discussions and assistance. This work was supported in part by NSF Grant No. MRSEC96-3252.

*Present address: Department of Physics, University of Pune, Pune 411007, India.

†Present address: Department of Material Science and Engineering, Shenzhen University, Shenzhen, Guangdong 518060, China.

‡Also at Department of Chemistry and Physics, Rowan University, Glassboro, NJ 08028-1701.

§Present address: Rochester Institute of Technology, Rochester, NY 14623.

[1] J.M.D. Coey, M. Viret, and S. Von Molnar, Adv. Phys. **48**, 167 (1999).

[2] A. Urushibara, Y. Moritomo, T. Arima, A. Asamitsu, C. Kido, and Y. Tokura, Phys. Rev. B **51**, 14 103 (1995).

[3] M. Dominguez, S.E. Lofland, S.M. Bhagat, A.K. Raychaudhuri, H.L. Ju, T. Venkatesan, and R.L. Greene, Solid State Commun. **97**, 193 (1996).

[4] University of Maryland, Technical Report 98-1 (unpublished).

[5] K. Takenaka, K. Iida, Y. Sawaki, S. Sugai, Y. Moritomo, and A. Nakamura, J. Phys. Soc. Jpn. **68**, 1828 (1999).

[6] Y. Moritomo, T. Akimoto, A. Nakamura, K. Ohoyama, and M. Ohashi, Phys. Rev. B **58**, 5544 (1998).

[7] H. Fujishiro, M. Ikebe, and Y. Konno, J. Phys. Soc. Jpn. **67**, 1799 (1998).

[8] S.I. Patil, S.M. Bhagat, S.B. Ogale, Q.Q. Shu, S.E. Lofland, and I.O. Troyanchuk, J. Appl. Phys. **87**, 5028 (2000).

[9] C.H. Chen and S-W. Cheong, Phys. Rev. Lett. **76**, 4042 (1996).

[10] H.L. Liu, S.L. Cooper, and S-W. Cheong, Phys. Rev. Lett. **81**, 4684 (1998).

[11] Y. Okimoto, T. Tomioka, Y. Onose, Y. Otsuka, and Y. Tokura, Phys. Rev. B **57**, R9377 (1998).

[12] Y. Okimoto, Y. Tomioka, Y. Onose, Y. Otsuka, and Y. Tokura, Phys. Rev. B **59**, 7401 (1999).

[13] S.E. Lofland, Q.Q. Shu, S.M. Bhagat, M.C. Robson, and R. Ramesh, Appl. Phys. Lett. **75**, 1947 (1999).

[14] S. Mori, C.H. Chen, and S-W. Cheong, Phys. Rev. Lett. **81**, 3972 (1998).

[15] G. Allodi, R. DeRenzi, F. Licci, and M.W. Pieper, Phys. Rev. Lett. **81**, 4736 (1998).

[16] M. Roy, J.F. Mitchell, A.P. Ramirez, and P. Schiffer, Phys. Rev. B **58**, 5185 (1998).
[17] J. Dho, I. Kim, and S. Lee, Phys. Rev. B **60**, 14 545 (1999).
[18] N. Fukumoto, S. Mori, N. Yamamoto, Y. Moritomo, T. Katsufuji, C.H. Chen, and S-W. Cheong, Phys. Rev. B **60**, 12 963 (1999).
[19] A. Moreo, S. Yunoki, and E. Dagotto, Science **283**, 2034 (1998).
[20] E.L. Nagaev, Phys. Lett. A **234**, 321 (1998).
[21] K.H. Kim, M. Uehara, C. Huse, P.A. Sharma, and S-W. Cheong, Phys. Rev. Lett. **84**, 2961 (1999).
[22] S.H. Chun, M.B. Salamon, and P.D. Han, Phys. Rev. B **59**, 11 155 (1999).
[23] J.C. Maxwell-Garnett, Philos. Trans. R. Soc. London, Ser. A **203**, 385 (1904).
[24] Z. Fang, I.V. Solovyev, and K. Terakura, Phys. Rev. Lett. **84**, 3169 (2000).